Journal of Electrical Engineering, Vol. 75, No. 4, 2024, pp. 258-267

sciendo
PAPERS

An optimized integral performance criterion based commercial PID controller design for boost converter

Mohammad Irshad[1], Naresh Kumar Vemula[2], Ramesh Devarapalli[3], Gundavarapu Venkata Nagesh Kumar[4], Łukasz Knypiński[5,*]

Boost converters often face challenges such as sluggish dynamic behavior, inadequate voltage regulation, and variations in input voltage and load current. These issues necessitate the need for closed-loop operation. Nature-inspired optimization algorithms (NIOA) have demonstrated their effectiveness in delivering enhanced solutions for various engineering problems. Several studies have been conducted on the use of proportional-integral-derivative (PID) controllers for controlling boost converters, as documented in the literature. Some studies have shown that using fractional order PID (FO-PID) controllers can lead to better performance than traditional PID controllers. Nevertheless, implementing FO-PID can be quite complex. Considering the widespread use of commercial PID controllers in industrial settings, this study focuses on finding the best tuning for these controllers in DC-DC boost converters. The approach used is particle swarm optimization (PSO) based on integral performance criteria. Simulation results indicate that the proposed controller achieves superior performance, evidenced by the lowest settling time, overshoot, integral absolute error (IAE), and integral squared error (ISE) values under varying input voltage and load current conditions, compared to both PID and FO-PID controllers. These findings have been confirmed through hardware implementation, which demonstrates the effectiveness of the proposed controller.

Keywords: DC-DC boost converter, optimal PID controller parameters, fractional order PID, ISA-PID, PSO

1 Introduction

The DC-DC converters are finding widespread use in many applications, such as LED lighting, medical instruments, defense equipment, photovoltaic applications [1], power factor correction circuits [2], electric vehicles [3], fuel cell applications [4], etc. The DC-DC boost converter is a system that exhibits a non-minimal phase. The presence of right-half plane (RHP) zero in the linearized model causes it to demonstrate an inverse response, which leads to instability with high gain and bandwidth limitation [5]. Furthermore, when operated in open-loop mode, the boost converter displays sluggish response and poor voltage regulation. Hence, closed-loop control is required to overcome these limitations.

A proportional-integral-derivative (PID) controller is widely used to date due to its simple control structure and ability to perform satisfactorily for a wide class of processes. Further, with the advent of nature-inspired optimization algorithms, their applications in many engineering problems led to better/improved solutions. Thus, researchers have proposed various design strategies based on these algorithms to tune PID for closed-loop control of boost converter [6-11]. In [6], a genetic algorithm (GA) for controller design is combined with the evolution of a queen bee in a hive to create a hybrid optimization method. It is shown that PID tuned with this modified algorithm performs better than GA-tuned PID. In [7], modified particle swarm optimization, termed as probabilistic particle swarm optimization (PSO) was employed to tune PID. The effectiveness of the proposed algorithm for controller design is verified experimentally. An algorithm based on a colony of foraging ants is used for controller design in [8]. The performance of the designed PID is compared with that of the tuned PID to achieve specified gain-phase margin specifications. Further, the simulation results were verified experimentally. In [9], three evolutionary algorithms (GA, differential evolution and artificial immune system) were employed to tune PID controller. It is shown through simulation results supported by experimental validation that optimally tuned PID has enhanced capability of output voltage regulation under different perturbations. The authors in

[1] Department of Electrical and Electronics Engineering, Saveetha School of Engineering, Saveetha Institute of Medical and Technical Sciences, Saveetha University, Chennai, India
[2] Department of Electrical and Electronics Engineering, SRM University AP, Andhra Pradesh – 522503, India
[3] Department of Electrical/Electronics and Instrumentation Engineering, Institute of Chemical Technology, Indianoil Odisha Campus, Bhubaneswar 751013, India
[4] Department of Electrical and Electronics Engineering, JNTUA Pulivendula, Andhra Pradesh – 516390, India
[5,*] Faculty of Automatic Control, Robotic and Electrical Engineering, Poznan University of Technology, 60-965 Poznan, Poland
* lukasz.knypinski@put.poznan.pl

https://doi.org/10.2478/jee-2024-0032, Print (till 2015) ISSN 1335-3632, On-line ISSN 1339-309X

[10] have merged Ziegler-Nichol's and optimization techniques to design a PID controller. In [11], the authors focused on enhancing the converter's performance and reducing voltage fluctuations through the utilization of PID controller that has been optimized with firefly algorithm.

Some reported works [12-19] have also designed a fractional order PID (FO-PID) controller for the control of boost converter using optimization algorithms. In [12], PSO was used to tune the fractional order PID by minimizing the weighted combination of ITAE and control input. Integral performance criteria, namely IAE was chosen for controller design and minimized by the artificial bee colony (ABC) algorithm in [13]. In [14], a multi-objective optimization approach was reported for controller design. A set of optimal gains were provided to choose proper value based on design requirements. It is observed that the optimal FO-PID controller gives improved performance in comparison to the optimal PID. In [15], the authors utilized Moth-Flame optimization (MFO) and PSO to fine-tune a fractional order fuzzy PID controller for a boost converter. The results indicated that there was an improved performance compared to fuzzy PID controller. In [16], the design and analysis for a boost converter and PV system controlled by the FO-PI were presented. The flower pollination algorithm (FPA) and water cycle algorithm (WCA) were used to tune the controller. Queen bee assisted genetic algorithm optimization was used to tune FO-PID controller in [17], and it was shown that it improved robustness compared to optimized PID. In [18], a novel topology for a FOPID controller was introduced for boost converter control. The controller's tuning was done using a combination of GA and integral performance criteria, specifically ITAE and ITSE. The proposed controller exhibits a wide operational range. Also, fuzzy FO-PID was designed to tackle robustness issues. In [19], Neural network combined with PSO was used to tune the controller gains for FO-PID.

Literature gap: as per the aforementioned literature, several authors have utilized FO-PID along with different optimization schemes to tune the controller gains. However, the use of commercial PID, also known as ISA-PID, has not been reported so far in the literature for controlling a boost converter to the best of the author's knowledge. The control structure of an ISA-PID is a two-degree-of-freedom (2-DOF) system that has the same number of controller parameters as FO-PID. One of its major advantages over FO-PID is its ease of implementation. The hardware circuit of ISA-PID is very simple and can be easily constructed. But FO-PID hardware circuit is complex and difficult to construct. Only approximate modeling can be done for FO-PID but actual modeling is possible in case of ISA-PID.

Hence, in the present work, a commercial PID controller is utilized and optimally tuned using particle swarm optimization [20] based on integral performance criteria for a DC-DC boost converter. Also, the efficacy of the proposed optimal scheme for closed-loop performance is compared with that of existing optimal PID and FO-PID controllers [21, 22]. The integral of the squared time-cubed weighted error (IST^3E) criterion is considered as an objective function. Furthermore, the PSO algorithm minimizes the objective function to get the optimal controller parameters for all three controllers. Duty cycle constraints have been handled during the design process for practical viability. Simulations performed on linearized averaged and switched models show that the proposed optimal ISA-PID observes notable improvement in performance.

2 Mathematical modelling of the DC-DC boost converter

Figure 1 shows a basic boost converter topology. State space averaging technique [23] is used to obtain a mathematical model of the boost converter. In the circuit, V_0, V_C, V_{in}, I_L, I_C, R, L, C, i_{load} represent the output voltage, capacitor voltage, input voltage, inductor current, capacitor current, load resistance, inductance, output capacitance, and perturbation in load current respectively. Here, the equivalent series resistance of the corresponding capacitor and inductor are ignored, and the small signal model is considered for continuous conduction mode for simplicity. The state equations for ON and OFF conditions are

$$L\frac{di_L}{dt} = v_{in} \tag{1}$$

$$C\frac{dv_c}{dt} = -\frac{v_c}{R} \qquad v_o = v_c \tag{2}$$

$$L\frac{di_L}{dt} = v_{in} - (1-d)v_o \tag{3}$$

$$C\frac{dv_c}{dt} = (1-d)i_L - \frac{v_c}{R} \qquad v_o = v_c \tag{4}$$

where d is the duty cycle.

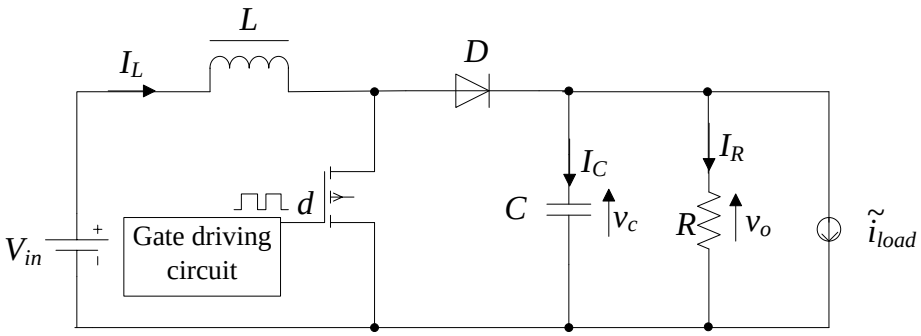

Fig. 1. DC-DC boost converter

Variables are perturbed about their steady state operating values as follows:

$$v_c = V_c + \tilde{v}_c \quad v_{in} = V_{in} + \tilde{v}_{in} \quad i_L = I_L + \tilde{\imath}_L \quad (5)$$

$$v_o = V_o + \tilde{v}_o \quad d = D + \tilde{d} \quad (6)$$

where symbols represented by uppercase letter and '~' are DC steady-state quantities and small perturbations, respectively.

Substituting (6) in (3) and (4), we get:

$$L\frac{d(I_L + \tilde{\imath}_L)}{dt} = (V_{in} + \tilde{v}_{in}) - (1 - D - \tilde{d}\,)(V_o + \tilde{v}_o) \quad (7)$$

$$C\frac{d(V_c + \tilde{v}_c)}{dt} = \left(1 - D - \tilde{d}\right)(I_L + \tilde{\imath}_L) - \frac{(V_c + \tilde{v}_c)}{R} - \tilde{\imath}_{load} \quad (8)$$

$$V_o + \tilde{v}_o = V_c + \tilde{v}_c \quad (9)$$

Considering only AC terms (neglecting second-order terms), the final dynamic (small AC signal) state space averaged model is obtained as follows:

$$L\frac{d\tilde{\imath}_L}{dt} = \tilde{v}_{in} - (1 - D)\,\tilde{v}_o + V_o\tilde{d} \quad (10)$$

$$C\frac{d\tilde{v}_c}{dt} = (1 - D)\,\tilde{\imath}_L - I_L\tilde{d} - \frac{\tilde{v}_c}{R} - \tilde{\imath}_{load} \quad 11)$$

$$\tilde{v}_o = \tilde{v}_c \quad (12)$$

By simplifying the above equations, the transfer function of the converter (linearized average model) can be obtained as follows.

Control-to-output transfer function

$$G_p(s) = \frac{\tilde{v}_o(s)}{\tilde{d}(s)} = \frac{(1 - D)\,V_o - LI_L s}{(LC)\,s^2 + \frac{L}{R}s + (1 - D)^2} \quad (13)$$

Line-to-output transfer function

$$G_p(s) = \frac{\tilde{v}_o(s)}{\tilde{v}_{in}(s)} = \frac{(1 - D)}{(LC)\,s^2 + \frac{L}{R}s + (1 - D)^2} \quad (14)$$

Output impedance transfer function

$$G_{dl}(s) = \frac{\tilde{v}_o(s)}{\tilde{\imath}_{load}(s)} = \frac{-Ls}{(LC)\,s^2 + \frac{L}{R}s + (1 - D)^2} \quad (15)$$

Putting parameter values chosen for the boost converter in (13), (14) and (15), we obtained:

$$G_p(s) = \frac{-1667s + 6 \times 10^7}{s^2 + 20s + 7.2 \times 10^5} \quad (16)$$

$$G_{dv}(s) = \frac{1.2 \times 10^6}{s^2 + 20s + 7.2 \times 10^5} \quad (17)$$

$$G_{dl}(s) = \frac{-1000s}{s^2 + 20s + 7.2 \times 10^5} \quad (18)$$

3 Integral performance criteria based controller design

The classical control structure as shown in Fig. 2 is utilized for the design of PID and FO-PID. $G_p(s)$, $G_{dv}(s)$ and $G_{dl}(s)$ are control-to-output, line-to-output and output impedance transfer functions, respectively. $G_c(s)$ is the respective controller; r, u, y, d_1 and d_2 are reference, control effort (duty cycle), output, load current disturbance and input voltage disturbance, respectively.

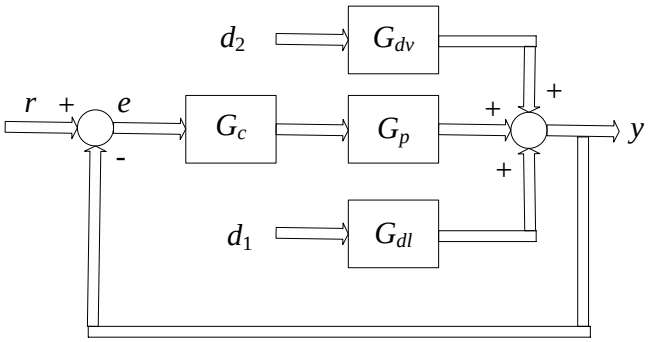

Fig. 2. Classical unity feedback control structure

The transfer functions of the PID and FO-PID are given below.

PID controller:

$$G_c(s) = K_c\left(1 + \frac{1}{\tau_i s} + \frac{\tau_d s}{0.1\tau_d s + 1}\right) \quad (19)$$

where K_c, τ_d, and τ_i are proportional gain, derivative time constant, and integral time constant, respectively.

FO-PID controller:

$$G_c(s) = K_c\left(1 + \frac{1}{\tau_i s^{\lambda}} + \tau_d s^{\mu}\right) \quad (20)$$

where λ and μ are fractional power of s. From, Fig. 2, error signals for the above two controllers for input voltage and load current disturbances are given by:

$$e_{dv} = -\frac{G_{dv}(s)}{1 + G_c(s)G_p(s)} d_2(s) \quad (21)$$

$$e_{dl} = -\frac{G_{dl}(s)}{1 + G_c(s)G_p(s)} d_1(s) \quad (22)$$

The well-known ISA-PID control law [24] is represented as:

$$u(s) = K_c\left[b\, r(s) - y(s) + \left(r(s) - y(s)\right)\frac{1}{\tau_i s} + \left(c\, r(s) - y(s)\right)\frac{\tau_d s}{1 + \frac{\tau_d s}{N}}\right] \quad (23)$$

where N is the ratio between τ_d and the first-order time constant of the filter cascaded with the derivative term, b and c are set-point weights and $r(s)$ is the reference signal. Rearranging (23) leads to control structure shown in Fig. 3, where G_{c1} and G_{c2} are characterized by the following transfer functions.

In order to have practical viability, constrained optimization ($0 \le \mu < 1$) is employed.

The IST^3E criterion [25-29] is chosen as an objective function. Mathematically, it is represented as:

$$IST^3E = \int_0^{\infty} [e(\alpha, t)\, t^3]^2 dt \quad (24)$$

where, α denotes the control parameters to be chosen to minimize IST^3E.

$$G_{c1}(s) = K_c\left(b + \frac{1}{\tau_i s} + \frac{c\tau_d s}{1 + \frac{\tau_d s}{N}}\right) \quad (25)$$

$$G_{c2}(s) = K_c\left(1 + \frac{1}{\tau_i s} + \frac{\tau_d s}{1 + \frac{\tau_d s}{N}}\right) \quad (26)$$

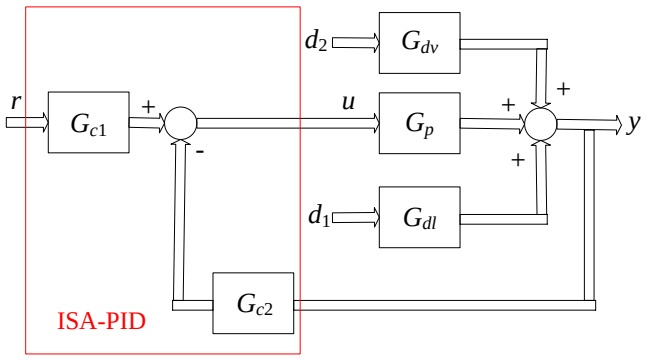

Fig. 3. The 2-DOF control structure representation of ISA-PID control law

The sum of errors due to both disturbances is included in the objective function for all the above three controllers. The classical PSO algorithm is used to minimize the chosen integral performance criterion to obtain optimal controller settings [30]. The optimization calculations are made for a swarm consisting of 50 particles. As a stop criterion was adopted the changes of the objective function for the best particle in successive iterations smaller than 3×10^{-4}. In order to obtain a good performance of the optimization procedure the specific parameters (w, c_1 and c_2) are adopted to optimized problem. The optimization calculations are made for the following parameters: w=0.35, c_1=1.1 and c_2=1.3. For brief understanding, the flowchart showing the various steps involved in PSO can be obtained from [31]. Table 1 shows the optimal controller parameter values of all three controllers. (Note: b and c are optimized for load disturbance rejection by keeping K_c, τ_i and τ_d values same as obtained with respect to set-point tracking).

Table 1. Optimal controller parameters

Controllers	K_c	τ_i	τ_d	λ	μ	b	c
PID	1.4×10^{-3}	5.4×10^{-4}	8.7×10^{-3}	-	-	-	-
FO-PID	5.9×10^{-3}	2.324×10^{-4}	1.14×10^{-5}	1.004	1.981	-	-
ISA-PID	8.86×10^{-2}	1.2×10^{-3}	1.178×10^{-4}	-	-	0.0028	0.014

4 Simulation results and experimental validation

4.1 Simulation parameters

The system parameters of the boost converter are tabulated in Tab. 2. The DC power supply and load are programmed to give perturbations in supply voltage and load current, respectively.

To compare the performance of the controllers designed in the previous section, simulations are performed on linearized averaged and switched models. Settling time (t_s), overshoot (O_s) (in percentage), IAE and ISE values are computed by perturbing load current and input supply voltage, which are mentioned in Tab. 3. (Note: Critically damped behavior is preferable for good design but response should settle as early as possible. Therefore, opting for underdamped design helps to reduce settling time but it should be achieved with minimum overshoot. Thus, opting for underdamped design with minimum overshoot together with reduction in settling time makes design more viable.)

Table 2. Performance measures for various controllers

Controller	**Input voltage disturbance**				**Load current disturbance**			
	t_s	O_s	IAE	ISE	t_s	O_s	IAE	ISE
PID	0.0151	24.864	0.112	0.783	0.035	1.400	0.0090	0.00397
FO-PID	0.0026	7.344	0.014	0.033	0.01382	0.806	0.0022	0.00063
ISA-PID	**0.0015**	**2.364**	**0.004**	**0.003**	**0.0041**	**0.199**	**0.0006**	**0.00007**

Table 3. Parameters of boost converter

Parameters	**Values**
V_{in}	30 V
V_o	50V
L	500 μH
C	1000 μF
D	0.40
R	50 Ω

4.2 Input voltage variation

To analyze the closed-loop performance, the input voltage is varied from 30 V to 37 V and then again from 37 V to 30 V. The output and control signals of various controllers for the linearized averaged model are illustrated in Fig. 4. From Fig. 5 and Tab. 3, it is observed that ISA-PID gives best disturbance rejection performance amongst all three controllers. The output signal settles in 0.00015 s which is the least as compared to PID and FO-PID. The percent overshoot is only 2.364 compared to FO-PID, which has a value of 7.344. IAE and ISE values also get reduced further with the use of ISA-PID. To show practical viability, switched and hardware model results are also taken. Figure 5 presents the output and control signals of PID, FO-PID, and ISA-PID for the switched model.

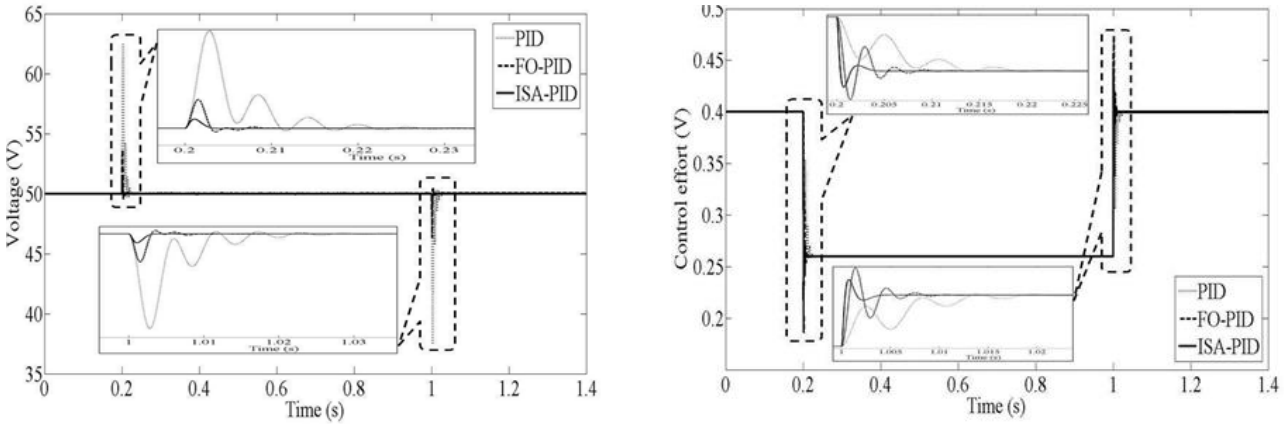

(a) (b)

Fig. 4. Linearized model when V_i is varied from 30 to 37 V at t=0.2 s and from 37 to 30 V at t=1.0 s: (a) output voltage (b) control signals

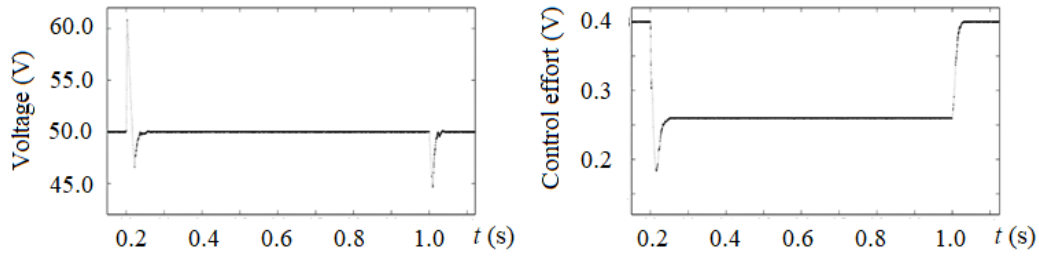

(a) PID

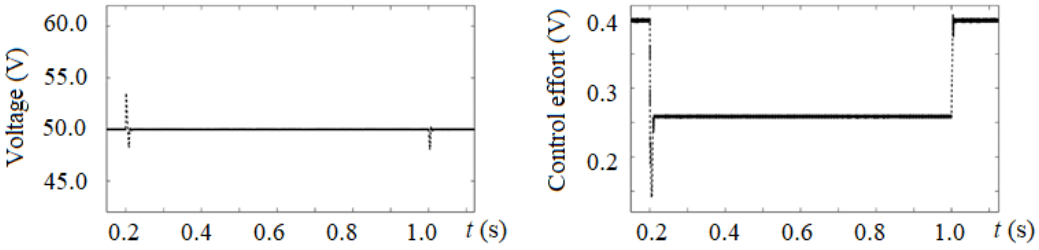

(b) Fractional PID

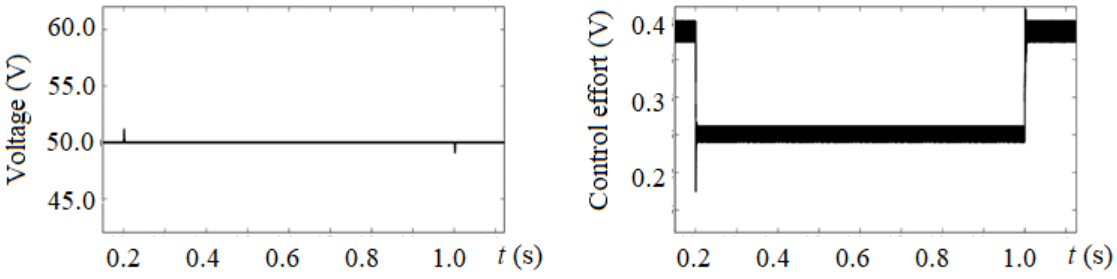

(c) ISA-PID

Fig. 5. Switched model output responses and control signals for input voltage disturbance of: (a) PID, (b) FO-PID, and (c) ISA-PID

4.3 Load current variation

The load resistance values are varied within the range of 25 Ω to 50 Ω and 50 Ω to 25 Ω to assess the effectiveness of the proposed model. The control effort and the output signals of various controllers for the linearized averaged model are illustrated in Fig. 6. It is observed from Fig. 6 that ISA- PID outperforms PID and FO-PID controllers. In the case of ISA-PID, the settling time value is reduced significantly. A minimum percent overshoot (%) is also observed. As far as IAE and ISE values are concerned, ISA-PID gives the least values amongst all the three controllers (Tab. 2). Figure 7 shows the output and control signals of various controllers for the switched model.

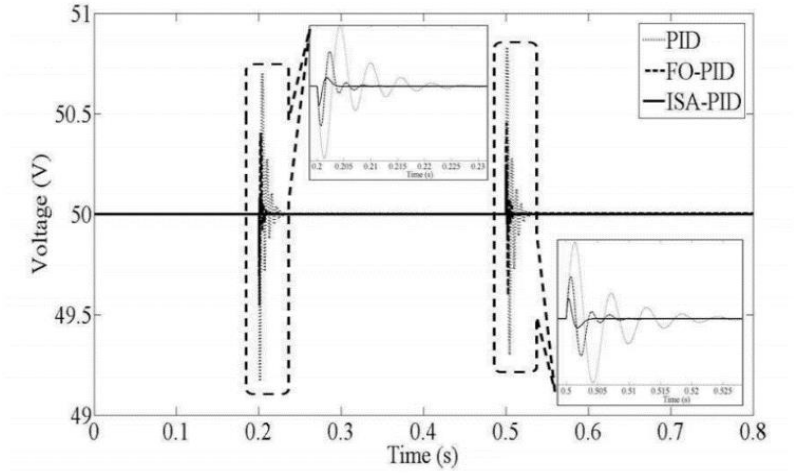

(a)

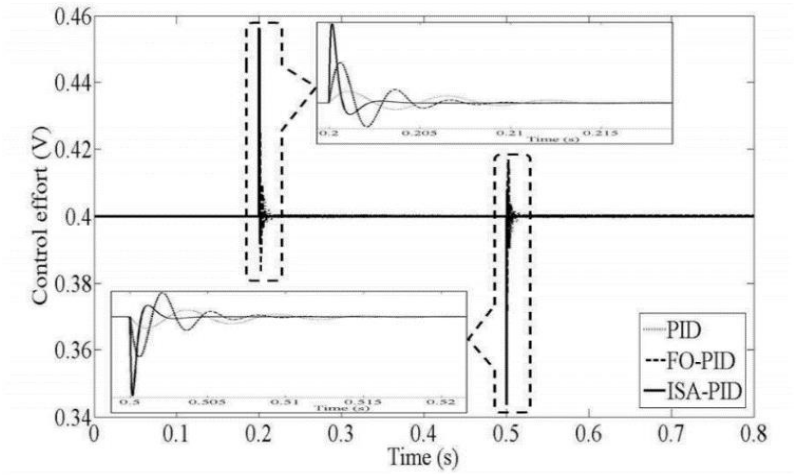

(b)

Fig. 6. Linearized model when R is changed from 50 to 25 Ω at t=0.2 s and from 25 to 50 Ω at t=0.5 s:(a) output response, and (b) control signals

From the above simulation results analysis, it is observed that commercial PID (control structure being used till date in industries) when optimized properly (in the present work) is sufficient for control of DC-DC boost converter, i.e. proves to be a better choice than fractional order PID and thus saves one from the complex implementation of FO-PID. Also, as the same existing control structure can be assimilated, saves the cost of new controller replacement in the industries.

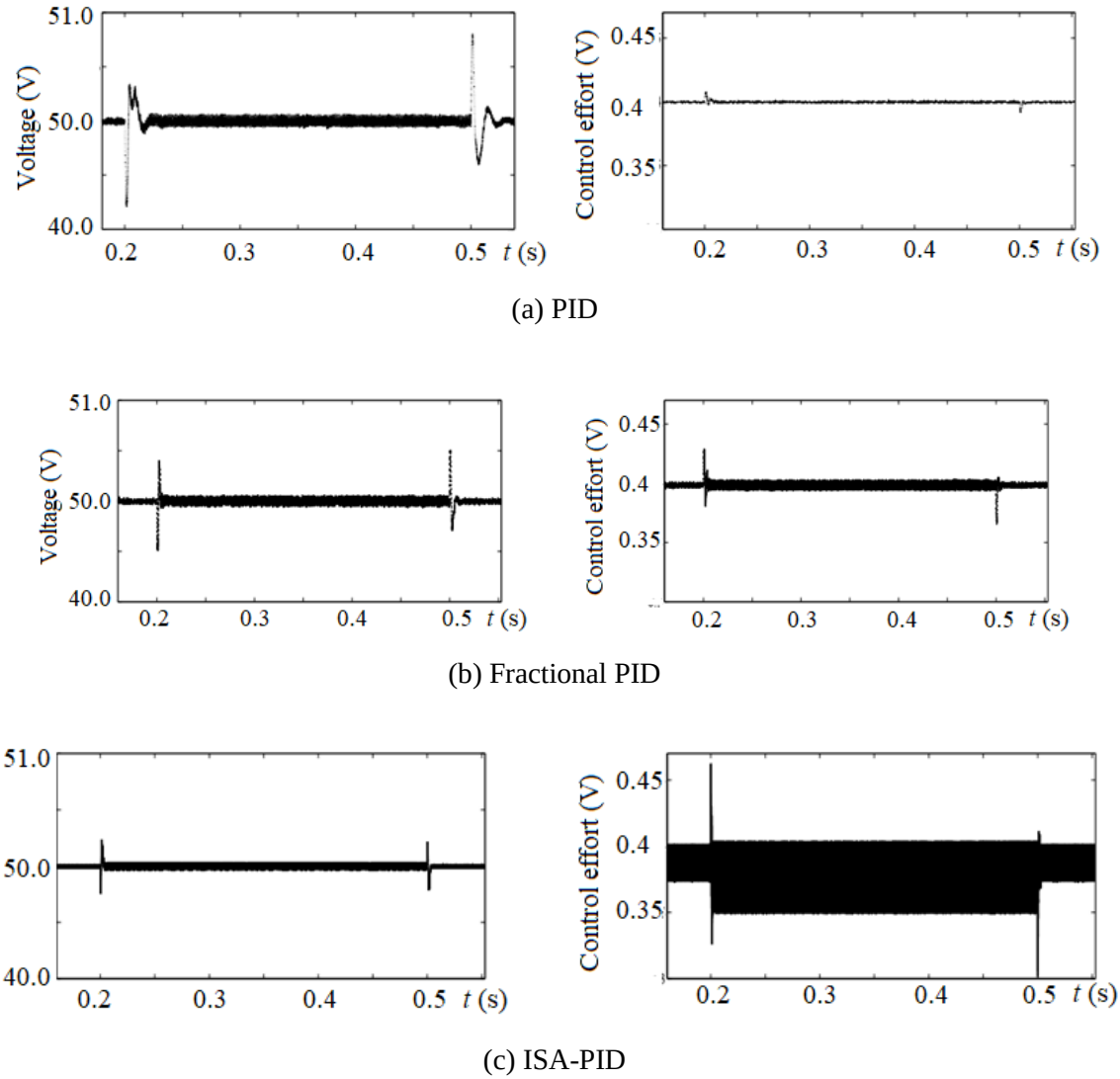

Fig. 7. Switched model output responses and control signals for load current disturbance of: (a) PID, (b) FO-PID, and (c) ISA-PID

5 Conclusions

DC-DC boost converter finds wide applications in day-to-day life. Closed-loop operation is required for regulated performance against input voltage and load current fluctuations. The use of PID and FO-PID controllers for the DC-DC boost converter is widely reported in the literature. In this work, the use of existing control structures in industries i.e. commercial PID (ISA-PID) controller is recommended against PID and FO-PID controllers for the control of DC-DC boost converter. Therefore, this work will be of keen interest for control practitioners and for those working towards finding feasible solutions for industrial problems. Using ISA-PID rather than PID and FO-PID will be in real sense a long-term solution. Though there can be different ways to properly tune ISA-PID, authors in the present work used integral performance criteria, one of popular approaches. All the parameters of ISA-PID are optimally tuned for the first time. To show the usefulness of the proposed design strategy, a comparative study has been done with PID and FO-PID by also optimally tuning both for the case of a linearized averaged model of the boost converter. For the case of input voltage disturbance, ISA-PID gives the shortest settling time value of 0.0015 s compared to FO-PID and PID having settling times as 0.0026 s and 0.0151 s respectively. Similarly, minimum overshoot (2.36%) is obtained with ISA-PID as compared to FO-PID (7.344%) and PID (24.86%). Also, minimum IAE (0.004) and ISE value (0.003) are exhibited by ISA-PID. For the case of load current disturbance, ISA-PID outperforms FO-PID and PID in all performance indices (Tab. 2). Switched model results are also provided to validate ISA-PID practical implementation on boost converter hardware circuitry.

The comparative study reveals the superiority of the proposed optimal ISA-PID over the other two controllers. Also, the use of ISA-PID will not only save the cost of purchase/replacement of a new controller but also substitute the complex implementation of FO-PID.

Acknowledgement

The authors are thankful to Indian institute of Technology Patna for carrying out the experimental validation of the proposed work.

References

[1] M. E. Sahin and F. Blaabjerg, "PV powered hybrid energy storage system control using bidirectional and boost converters", *Electric Power Components and Systems*, vol. 49, no. 15, pp. 1260-1277, 2022

[2] O. Aissa, S. Moulahoum, H. Talhaoui, B. Babes and A. Kessal, "Experimental validation of the boost power factor corrector converter based on smart intuitive control law", *Electric Power Components and Systems*, vol. 50, no. 4-5, pp. 1-13, 2022.

[3] M. A. Rodrıguez, "Parallel fault- tolerant and robust boost converter for vehicle-to-aid services", *Electric Power Components and Systems*, vol. 49, pp. 1463-1474, 2022.

[4] H. Djoudi, N. Benyahia, A. Badji, A. Bousbaine, R. Moualek, S. Aissou and N. Benamrouche, "Simulation and experimental investigation into a photovoltaic and fuel cell hybrid integration power system for a typical small house application", *Electric Power Components and Systems*, vol. 48, no. 14-15, pp. 1598-1613, 2020.

[5] J. Freudenberg and D. Looze, "Right half plane poles and zeros and design tradeoffs in feedback systems", *IEEE Trans. on Automatic Control*, vol. 30, no. 6, pp. 555-565, 1985.

[6] M. Mangaraj, J. Sabat and A. Kumar Barisal, "Experimental test performance for a comparative evaluation of a voltage source inverter: Dual voltage source inverter", *Journal of Electrical Engineering*, vol. 75, no. 1, pp. 56 - 62, 2024.

[7] K. Sundereswaran and V. Devi, "Application of a modified particle swarm optimization technique for output voltage regulation of boost converter", *Electric power Components and systems*, vol. 39, no. 3, pp. 288-300, 2021.

[8] K. Sundareswaran and V. Devi, "Feedback controller design for a boost converter through a colony of foraging ants", *Electric Power Components and Systems*, vol. 40, no. 6, pp. 672-690, 2012.

[9] K. Jayaswal, D. K. Palwalia and J. M. Guerrero, "A Comprehensive Performance Analysis of a 48-Watt Transformerless DC-DC Boost Converter Using a Proportional-Integral-Derivative Controller with Special Attention to Inductor Design and Components Reliability". *Technologies*, vol. 12, no. 18, 2024.

[10] G. Abbas, M. Adnan Samad, J. Gu, M. Usman Asad and U. Farooq, "Set-point tracking of a dc-dc boost converter through optimized PID controllers", *IEEE Canadian Conference on Electrical and Computer Engineering (CCECE)*, pp. 1-5, 2016.

[11] A. Izza et al., "Optimization DC-DC boost converter of BLDC motor drive by solar panel using PID and firefly algorithm", *Results in Engineering*, vol. 21, 2024.

[12] Jun-Yi Cao and Bing-Gang Cao, "Design of fractional order controllers based on particle swarm optimization", *1ST IEEE Conference on Industrial Electronics and Applications*, pp. 1-6, 2006.

[13] F. Merrikh-Bayatnad and S. Jamshidi, "Comparing the performance of optimal PID and optimal fractional-order PID controllers applied to the nonlinear boost converter", arXiv:1312.7517, pp. 1-6, 2013.

[14] A. Amirahmadi, M. Rafiei, K. Tehrani, G. Griva and I. Batarseh, "Optimum design of integer and fractional-order PID controllers for boost converter using SPEA look-up tables", *Journal of Power Electronics*, vol. 15, no. 1, pp. 160-176, 2015.

[15] A. Bennaoui, S. Saadi and A. Ameur, "Performance comparison of mfo and pso for optimal tuning the fractional order fuzzy PID controller for a dc-dc boost converter", *2020 International Conference on Electrical Engineering (ICEE)*, pp. 1-5, 2020.

[16] A. Mohamed, M. Mahmoud, R. A. Swief, L. Said and A. Radwan, "Optimal fractional-order PI with dc-dc converter and PV system", *Ain Shams Engineering Journal*, vol. 12, no. 2, pp. 1895-1906, 2021.

[17] S. V. Devaraj, M. Gunasekaran, E. Sundaram, M. Venugopal, S. Chenniappan, D. J. Almakhles, U. Subramaniam and M. S. Bhaskar, "Robust queen bee assisted genetic algorithm (qbga) optimized fractional order PID (FOPID) controller for not necessarily minimum phase power converters", *IEEE Access*, vol. 9, pp. 93331-93337, 2021.

[18] W. Yi, H. Ma, S. Peng, D. Liu, Z. Ali, U. Dampage and A. Hajjiah, "Analysis and implementation of multi-port bidirectional converter for hybrid energy systems", *Energy Reports*, vol. 8, pp. 1538-1549, 2022.

[19] M. Abdollahzadeh, H. Mollaee, S. M. Ghamari and F. Khavari, "Design of a novel robust adaptive neural network-based fractional-order proportional-integrated-derivative controller on DC/DC boost converter", *Journal of Engineering*, vol. 2023, no. 4, e12255.

[20] Ł. Knypiński, "Performance analysis of selected metaheuristic optimization algorithms applied in the solution of an unconstrained task", *COMPEL*, vol. 41, no. 5, pp. 1271-1284, 2022.

[21] R. Stanislawski, J. R. Tapamo and M. Kaminski, "A Hybrid Adaptive Controller Applied for Oscillating System", *Energies*, vol. 15, no. 6265, 2022.

[22] N. Ram Babu, T. Chiranjeevi, R. Devarapalli, Ł. Knypiński and F. P. Garcia Marquez, "Real-time validation of an automatic generation control system considering HPA-ISE with crow search algorithm optimized cascade FOPDN-FOPIDN controller", *Archives of Control Sciences*, vol. 33, no. 2, pp. 371-390, 2023.

[23] R. Erickson and D. Maksimovic, "Fundamentals of power electronics", Springer Science & Business Media, 2007.

[24] K. J. Astrom and T. Hagglund, "PID controllers: theory, design, and tuning", *Instrument society of America Research Triangle Park*, NC, 1995.

[25] A. Ali and S. Majhi, "Integral criteria for optimal tuning of PI/PID controllers for integrating processes", *Asian Journal of Control*, vol. 13, no. 2, pp. 328-337. 2011.

[26] M. Irshad and A. Ali, "Optimal tuning rules for PI/PID controllers for inverse response processes", *IFAC-PapersOnLine*, vol. 51, no. 1, pp. 413-418, 2018.

[27] A. Mitov, T. Slavov and J. Kralev, "Robustness Analysis of an Electrohydraulic Steering Control System Based on the Estimated Uncertainty Model", *Information*, vol. 12, no. 512, pp. 1-12, 2021.

[28] G. Zhao and H. Li, “Robustness analysis of logical networks and its application in infinite systems”, *Journal of the Franklin Institute*, vol. 357, no. 5, pp. 2882-289, 2020.

[29] N. R. Babu, T. Chiranjeevi, R. Devarapalli and S. K. Bhagat, "Optimal location of FACTs devices in LFC studies considering the application of RT-Lab studies and emperor penguin optimization algorithm", *Journal of Engineering Research*, vol. 11, no. 2, 100060, 2023.

[30] M. S. Alvarez-Alvarado, F. E. Alban-Chacón, E. A. Lamilla-Rubio, C. D. Rodríguez-Gallegos and W. Velásquez, "Three novel quantum-inspired swarm optimization algorithms using different bounded potential fields", *Scientific Reports*, vol. 11, no. 11655, pp. 1-22, 2021.

[31] D. Wang, D. Tan and L. Liu, “Particle swarm optimization algorithm: an overview”, *Soft Computin*g, vol. 22, pp. 387-408, 2017.

Received 14 May 2024